CFSRC COLLOQUIUM

Proceedings of the Cold-Formed Steel Research Consortium Colloquium
20-22 October 2020 (cfsrc.org)

The Direct Strength Method for Combined Bending and Web Crippling of Second-Generation Trapezoidal Steel Sheeting

Willems, D.W.C.[1], Hofmeyer, H.[2], Snijder, H.H.[3], Schafer, B.W.[4]

Abstract

Second-generation trapezoidal sheeting, characterised by longitudinal stiffeners in webs and flanges, is loaded near a support by a concentrated force and a bending moment. Currently, design codes predict related failure by: (a) determining the ultimate bending moment via the effective width approach or the Direct Strength Method (DSM); (b) finding the web crippling load via a curve-fitted formula; and (c) using an interaction rule to take into account the load combination. However, the effective width approach is quite complex to use for many longitudinal stiffeners, and the accuracy of the design code approach is subjected to improvement. Moreover, nowadays the DSM provides a consistent and well-established method to predict ultimate loads for cold-formed steel structures. Therefore, in this paper the application of DSM for combined bending and web crippling of second-generation sheeting is investigated. First a set of internationally representative second-generation trapezoidal sheeting types is used to create a set of numerical experiments, where sheet-sections are subjected to a three-point bending test. Then finite element models are developed and verified, and used to predict the buckling, yield and ultimate loads for the set of numerical experiments. With the results from the numerical experiments, an explicit DSM approach is developed, which predicts the ultimate load for combined actions directly. Hereafter, also an interaction DSM approach is studied, which first predicts the ultimate bending moment by the DSM, then the web crippling load by the DSM and then uses a classic interaction rule for the load combination. The explicit and implicit DSM approaches perform equally well, with a coefficient of variation equal to 0.13. The interaction DSM approach resembles the current design rules most and is therefore the preferred approach, although the explicit DSM approach is more direct and certainly deserves consideration too.

1. Introduction

Cold-formed thin-walled trapezoidal steel sheeting is widely used in the building industry for cladding (walls) and sheeting (roofs), where it is often used over multiple spans, resulting in a concentrated load and a bending moment above the intermediate supports. Trapezoidal sheeting can be classified into three categories, as shown in figure 1. For *first-generation* trapezoidal steel sheeting, prediction of the related failure load above the support can be carried out by several methods: (i) via the current design rules, based on partly theoretical models and curve-fitting of test results; (ii) the ultimate failure model [1]; and (iii) by an explicit or interaction Direct Strength Method (DSM) approach [2].

There are several issues related to the current design rules. The effective width method, used within the design codes to determine the ultimate bending moment, does not take interaction into account between the flanges and the web.

Furthermore, research in 2000 [1] showed that the design rules differ in their predictions seriously for first-generation trapezoidal steel sheeting. One of the possible causes for this is that the design rules are not fully based on physical models, but partly on curve fitting of test results.

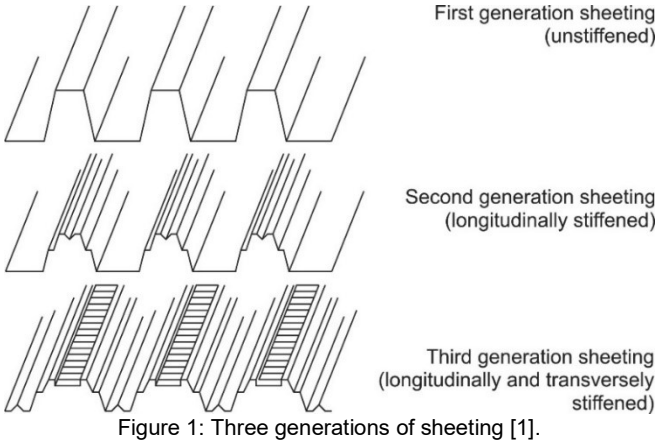

Figure 1: Three generations of sheeting [1].

[1] Graduate student, Department of the Built Environment, Eindhoven University of Technology, d.w.c.willems@alumnus.tue.nl
[2] Associate professor, Department of the Built Environment, Eindhoven University of Technology, h.hofmeyer@tue.nl
[3] Professor of Structural Design, Department of the Built Environment, Eindhoven University of Technology
[4] Professor of Civil & Systems Engineering, Department of Civil & Systems Engineering, Johns Hopkins whiting school of engineering

The before mentioned issues for the design rules still apply for second-generation sheeting. Additionally, the calculation of the effective cross-section, as needed for the effective width method, is increasingly difficult due to the longitudinal stiffeners in webs and flanges. A possible alternative for the design rules could then be the ultimate failure model. The ultimate failure model uses Marguerre's equations [3] to predict the plate behaviour due to the compressive forces of the bending moment up to failure. However, this model was too complex to use in practice, so a simplification by using a two-strip/fictitious strain method was introduced [4]. Both methods cannot be easily extended for application to longitudinally stiffened plates. As the DSM does not have these disadvantages, it is of interest to investigate whether the DSM can be used for second-generation sheeting. Even more so because the DSM showed to be successful for the predication of the ultimate load of first-generation sheeting [2].

In order to study and model the behaviour of second-generation sheeting, in this case with the DSM, always reference should be made to real experiments. Second-generation sheeting is much more used in practice then first-generation sheeting, while less experiments and simulations have been carried out. In 2002, a limited number of experiments were carried out to explore the differences in behaviour between first and second-generation sheeting [5]. The main conclusion was that the ultimate failure model could not be used for second-generation sheeting without significant adjustments. Franco and Batista [6] tried to find the optimised cross-section shapes to resist flexural buckling, resulting in the presentation of key design variables. The research confirmed that the geometry of the intermediate stiffeners is much more relevant for the buckling behaviour than the stiffeners' widths and the angles between web and flange. Finally, Caseriego et al. [7,8] investigated the application of Yield Line Theory (YLT) for first and second generation steel sheeting under pure compression or bending. Framed by the aforementioned research, in this paper the application of the DSM to combined bending and web crippling of second-generation sheeting is investigated.

3. Numerical experiments

To develop a set of numerical experiments that represents the situation in practice, table 1, commercially available second-generation trapezoidal steel sheeting is listed in table 2, as available in four countries: (i) The Netherlands; (ii) Australia; (iii) The United Kingdom; and (iv) The United States. These sheeting types are categorized with regards to the number of stiffeners in the web and flange. The recommended multi span length has been retrieved from the manufacturers' documentation and is converted to span lengths for an equivalent three-point bending simulation. To allow for variation, eight different span lengths are chosen for the simulations. The load bearing plate length (L_{lb}) varies between 40 and 160 mm. For each span length several load bearing plate lengths are present and the extreme cases, upper right corner and lower left corner of table 1, are excluded because they are unlikely to occur in practice. In table 1, every simulation is defined by a number, which is referring to a sheeting type via table 2. The variables S_f and S_w indicate the number of stiffeners in the flange and web respectively.

Table 1: Numerical experiments.

		L_{lb}	40			80		100		120			160		
		S_f	1	2	3	1	2	1	2	1	2	3	1	2	3
L_{span}	S_w														
600	0		1	2-3	4		6-7		8-10						
	1			5											
1000	0		11	12-13	14	15-16	17-20		22-24	26-27					
	1					21			25		28				
1200	0		29				30	32-34	35-37		39-41				
	1						31	38						42-43	
1400	0		44												
	1						46			50					
	2		45			47		48	49				51		
1800	1							54		55					
	2			52			53			56				57	
2200	1									61					
	2					58		59	60	62	63				64
2400	1												69		
	2							66	67		68				70
	3						65								
2800	2									72		73		74	
	3								71					75	

Table 2: Second-generation sheeting as available in the USA, UK, Australia (AU), and The Netherlands (NL).

Category	Manufacturer	Sheeting type	Country	Recommended multi span length [m]	Eq. span length for bending test [mm]	Simulation # (see table 1)	f_y [N/mm^2]
W0-F1	SAB	30KD/1050-S	NL	1-2.5	1000, 1200	26, 32	320
	SAB	58KD/945-S	NL	1-3.3	1200, 1400	29, 44	320
	SAB	50R/1000	NL	1-2.8	1000, 1200	27, 33	320
	SAB	35R/1035	NL	1-1.8	600, 1000	01, 11, 15	320
	Fielders	TL-5	AU	1-2.6	1000, 1200	16, 34	550
W0-F2	SAB	40R/915	NL	1-2.0	600, 1000	02, 12, 19	320
	SAB	45KD/1000	NL	1-2.8	1000, 1200	20, 37	320
	ArcelorMittal	39/333-3T	NL	1-2.0	600, 1000, 1200	03, 13, 30	320
	Accord	333 (35/1000)	UK	1-2.4	600, 1000, 1200	06, 17, 35	220
	Accord	BW32/1000	UK	1-2.4	600, 1000, 1200	07, 18, 36	220
	TTP	1000-32 Forward	UK	1-2.4	600, 1000, 1200	08, 22, 39	220
	TTP	1000-20 Liner	UK	1-2.4	600, 1000, 1200	09, 23, 40	220
	Accord	BW5RS/1000	UK	1-2.4	600, 1000, 1200	10, 24, 41	220
W0-F3	Lysaght	Multiclad (840)	AU	1-1.8	600, 1000	04, 14	550
W1-F1	SAB	85R/1120	NL	2-5.0	1400, 1800	50, 54	320
	SAB	106R+/750	NL	3-6.5	2200, 2400	61, 69	320
	SAB	70R/800	NL	2-5.0	1400, 1800	51, 55	320
	ArcelorMittal	37/250-4T	NL	1-2.5	1000, 1200	21, 38	320
W1-F2	Lysagth	Klip-lok classic 700	AU	1.6-3	1000, 1200	25, 42	550
	Fielders	Kingklip 700	AU	1-2.8	600, 1000, 1200	05, 28, 43	550
	Lysagth	Klip-lok classic 406	AU	1-3.6	1200, 1400	31, 46	550
W2-F1	SAB	153R/840	NL	4-7.8	2400, 2800	67, 74	320
	SAB	158R/750	NL	5-8.5	2400, 2800	66, 72	320
	SAB	100R/825	NL	3-5.5	1400, 1800, 2200	48, 56, 62	320
	Verco decking	PLW2 / W2 Formlock	USA	2.5-6	1400, 1800, 2200	45, 52, 58	345
	Verco decking	PLW3 / W3 Formlock	USA	2.5-6	1400, 1800, 2200	47, 53, 59	345
W2-F2	ArcelorMittal	135/310-3T	NL	4-7.0	2200, 2400	60, 68	320
	SAB	89R/915	NL	2-5.3	1400, 1800, 2200	49, 57, 63	320
W2-F3	ArcelorMittal	106/250-3T	NL	3-6,5	2200, 2400, 2800	64, 70, 73	320
W3-F2	ArcelorMittal	200/420-2T	NL	6-9.5	2400, 2800	65, 71, 75	320

4. Finite element simulations

4.1 Sheeting geometry

To make the modelling of all the different second-generation sheeting types efficient in the finite element method, a parametric model has been defined in Python [9]. The Python script is based on a basic model of the cross-section with stiffeners as presented in figure 3 (due to symmetry only half top and bottom flanges are shown). The model can handle a maximum of three stiffeners for each flange or web. Fewer stiffeners are enabled by setting the non-existing stiffeners' dimensions to zero.

4.2 Simulation approach

Figure 2 shows an overview of the finite element simulation approach. The FEM C_{NL} model (Combined bending and web crippling, Non-Linear analysis) provides the P_u (ultimate load) and P_y (yield load) for the numerical experiments. IN a similar vein, the C_{MOD} model (Combined bending and web crippling, MODal analysis) generates the P_{cr} (buckling load). An explicit DSM-C equation can be derived using the P_u, P_y and P_{cr} loads and will determine a prediction for the ultimate load $P_{u;DSM}$. Similar to the C_{NL} and C_{MOD} models, finite element models are made for pure bending (models B_{NL} and B_{MOD}), and IOF or ITF web crippling (W_{NL} and W_{MOD}). The interaction DSM approach is developed by DSM equations for pure bending and web crippling, which can be used in combination with an interaction rule. In the end, both the explicit and interaction DSM approaches can be evaluated by their Coefficient of Variation (CoV) to P_u, which has been obtained by the C_{NL} model.

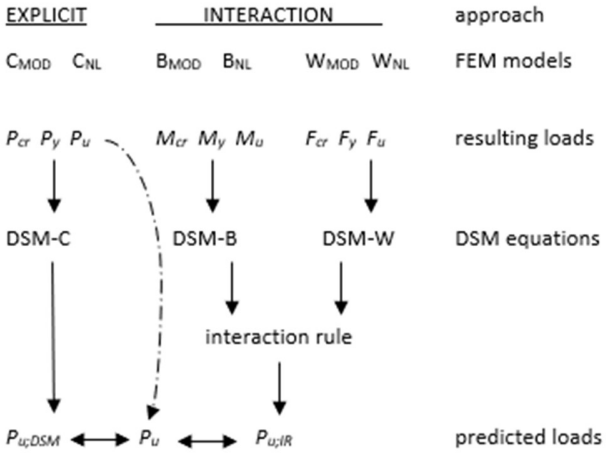

Figure 2: Several FEM models (top row) are used for the numerical experiments to produce the data for the DSM approaches.

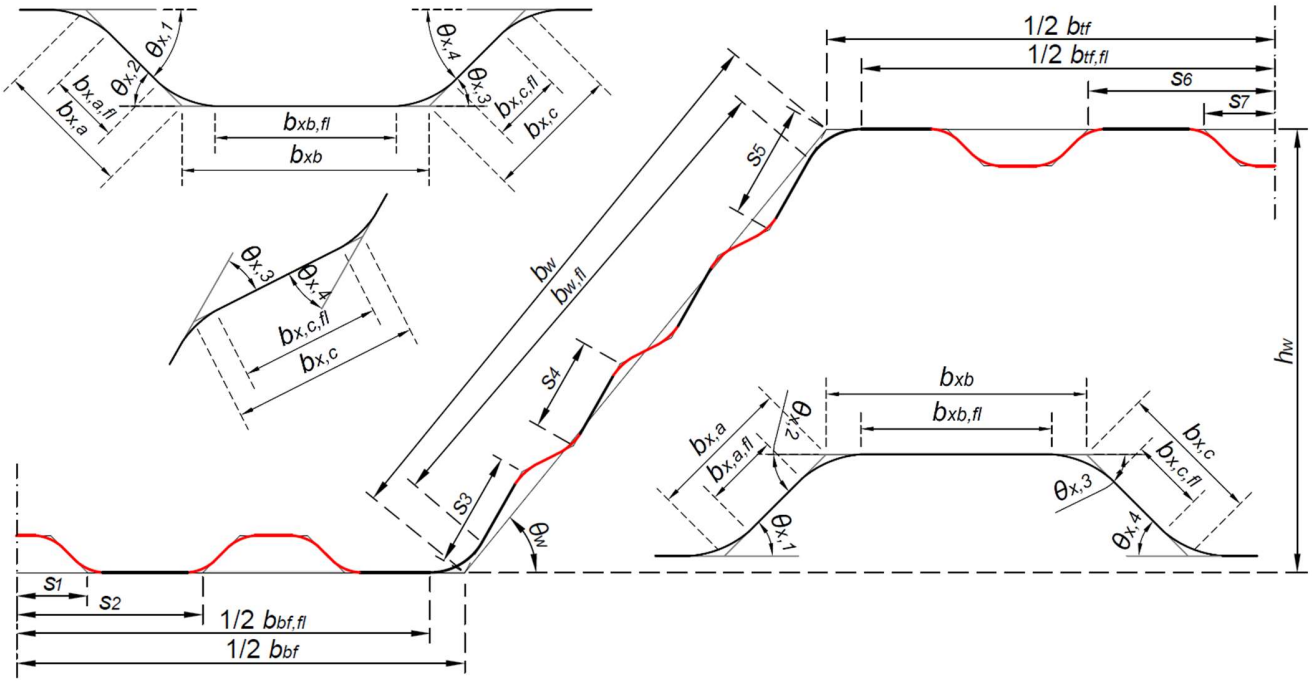

Figure 3: FEM geometry model with (the maximum number of) stiffeners shown in red.

4.3 FEM setup

The finite element models are a further development of existing models for first-generation sheeting [2], and have been developed in Abaqus 6.14 [9]. Due to the possibility of asymmetric failure behaviour (in length direction), half of the sheet-section is modelled, as shown in figure 4.

The C_{NL} model consists of two parts: the sheet-section modelled by four-node shell elements with reduced integration and hourglass control, and the load bearing plate made by rigid shell elements. Frictional interaction exists between the sheet-section and the load-bearing plate, formulated by standard "surface-to-surface contact" in Abaqus [9]. Symmetry boundary conditions, the supports, the strips preventing spreading of the webs, and the boundary conditions of the load bearing plate have been modelled similar to the models of first-generation sheeting [2] and are shown in figure 4.

Mesh densities are very similar to the models for first-generation too [2]. The finest mesh is located at mid-span and the mesh gradually evolves to a coarse mesh, see figure 5. The mesh size used for the flat parts of each stiffener follows the mesh in the same region. The finite element models for pure bending are meshed with a global mesh size, following the constant stress gradients over the length. The compressed flange corner was meshed with at least three elements tangentially, and increased to five elements for corner radii larger than 6 mm.

For the other models C_{MOD}, B_{NL}, B_{MOD}, W_{NL}, and W_{MOD}, adaptations are made to the C_{NL} model. For the modal analyses, the load-bearing plate is replaced by two unit loads at the junction between the compressed flange and its corner, at an in-between distance equal to the load bearing plate width. In case of the IOF and ITF web crippling models, the span length is adjusted to follow the requirements of the AISI S100-16 [10]. For the pure bending models, the load bearing plate is replaced by a prescribed rotation R_x of the supports. For the B_{NL} model, the first positive Eigenmode from the B_{MOD} model is used as an imperfection, with its maximal amplitude equal to 1/1000 of the compressed flange width. For all models, an implicit dynamic solving procedure is used, in which the total applied deformation of -25 mm takes place within 1 s. Further solution settings are taken from the previous models [2].

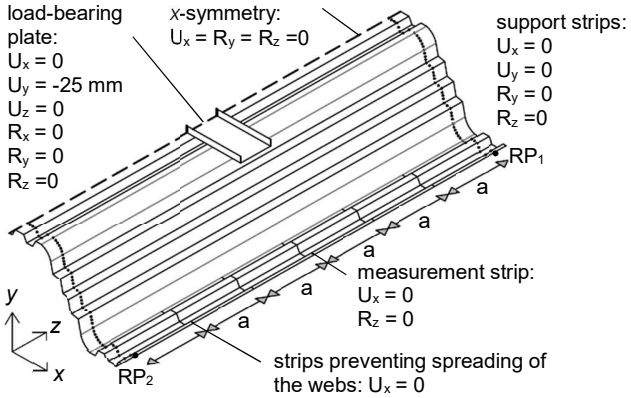

Figure 4: Boundary conditions for finite element model C_{NL}.

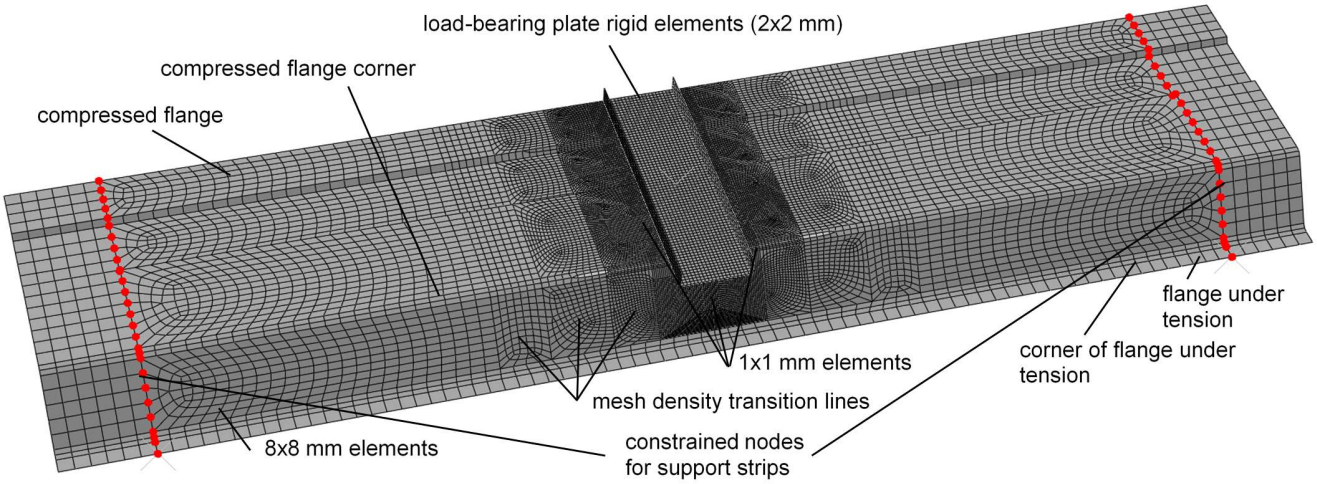

Figure 5: Mesh of finite element model C_{NL}

4.4 Verification

Verification of the finite element models was carried out by comparing the results of the C_{NL} model with experiments carried out in 2002 [5] and with previous simulations of these experiments by Vervoort [11]. Figure 6 presents the Pearson product-moment correlation coefficient (ρ), the average and Coefficient of Variation (CoV) of the ultimate loads as found for the experiments ($P_{u,EXP}$) and as predicted by the C_{NL} model (P_u) (black markers), and similar for the ultimate load as predicted by the previous simulations $P_{u,SIMV}$ and the C_{NL} model (red markers). Additionally, the load-beam deflection, load-web crippling deformation, and support-web crippling deformation graphs, and the post-failure modes as found with the C_{NL} model were compared to the experiments and previous simulations. For all these above aspects, a good resemblance was found, which verifies the new finite element model C_{NL} to be used in this paper.

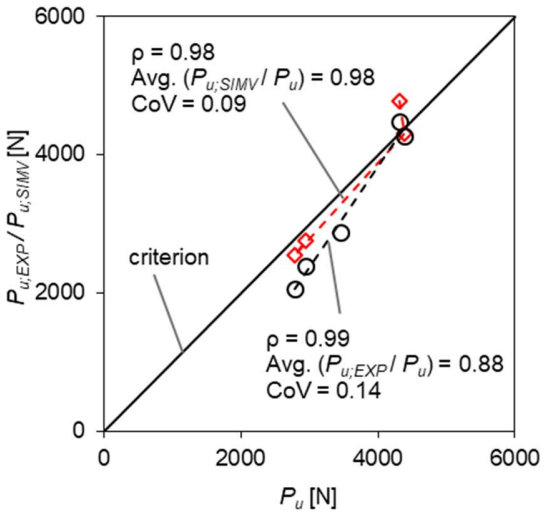

Figure 6: C_{NL} ultimate loads P_u vs. experimental loads $P_{u;EXP}$ (black markers) and previous simulations by Vervoort $P_{u;SIM}$ (red markers)

4.5 Results

If the C_{NL} finite element model is used to carry out the numerical experiments, as given in table 1, all the post-failure modes that occur can be interpreted as one of the three post-failure modes that were found for first-generation sheeting. Also, corresponding load-web crippling deformation diagrams show that the characteristics of these curves are similar to those of first-generation sheeting.

Using the finite element models as presented in figure 2 for the numerical experiments in table 1, the ultimate load, the yield load, and the first positive Eigenvalue (buckling load) are determined. The yield load is predicted by the first occurrence of plastic dissipation, taking into account the whole model, and measured both at the membrane surfaces and the outer surfaces of the shell elements. For the pure bending simulations, the yield "load" (i.e. bending moment) is determined by a linear elastic simulation, in accordance with the DSM guidelines in AISI-S100-16 [10]. The generated data will be used in the next section to develop the DSM approaches.

5. Direct Strength Method

5.1 Explicit DSM approach

In general, to calibrate a DSM equation, three loads are required: (i) the ultimate load (P_u); (ii) a buckling load (P_{cr}); and (iii) a yield load (P_y). Note that for the variable P also M or F can be used. For the format of a DSM equation, many different versions are given in literature. Here, equations (2) till (7) from the research on the DSM of first-generation trapezoidal steel sheeting are selected [2]. The k_i factors in the equations (see [2]) are determined such that the mean of the squared errors between the normalized ultimate loads from the finite element model and the DSM equation is minimal. For the explicit DSM approach, the best performing equations is found to be equation (7) in ref [2], for which the coefficient of variation (CoV) is 0.13, see figure 7.

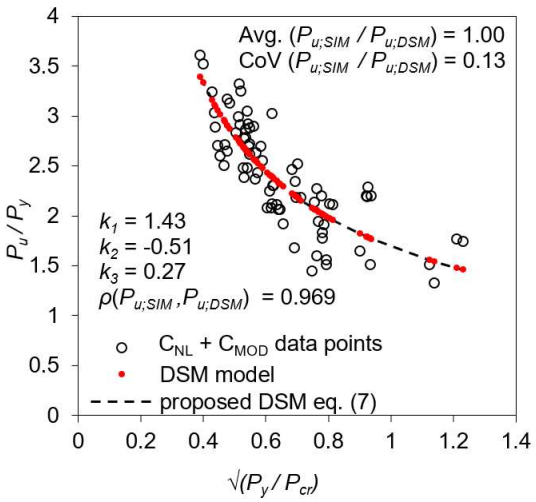

Figure 7: DSM-C; equation 7 [2] for combined bending and web crippling. Dotted line shows DSM model for all values of slenderness.

5.2 Explicit DSM approach with linear elastic determined yield loads

For the yield load, the load at which first plastic dissipation occurs in the geometric and material non-linear simulation was used. However, in case of pure bending, the first yield load (moment) is determined by a linear elastic simulation. For simulations 4,14, 31, and 36 the yield load exceeds the first positive Eigenvalue, which means instabilities may occur here before the yield load. Therefore, for all simulations a linear elastic determined yield load is obtained as follows:

$$P_{y\_LE} = \frac{f_y}{f_{10\%}} P_{u10\%} \qquad (1)$$

with $P_{u10\%}$ equal to 10% of the ultimate load; f_y the yield stress; $f_{10\%}$ the maximum Von Mises stress at 10% of the ultimate load and P_{y_LE} the linear elastic determined yield load. Following the same approach as presented in section 5.1, but now using the linear elastic determined yield load, results in virtually the same performance, see figure 8.

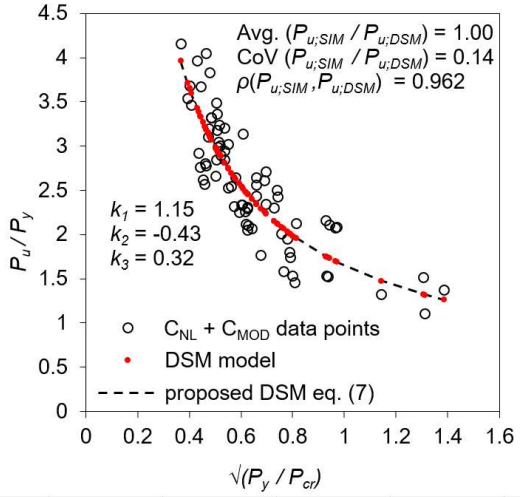

Figure 8: DSM-C; equation 7 [2] for combined bending and web crippling with a linear elastic determined yield load

5.3 Interaction DSM approach

The interaction DSM approach first predicts the ultimate bending moment (by fitting the pure bending simulations), then the web crippling load (in this section by IOF simulations), and then uses an interaction rule for combined actions. For the pure bending simulations, the DSM-B (B stands for bending) equation (7) [2] resulted in the highest performance, figure 9. However, for the IOF web crippling simulations, DSM-W (W for web crippling) equation (5) [2] resulted in the lowest CoV = 0.12, see figure 10.

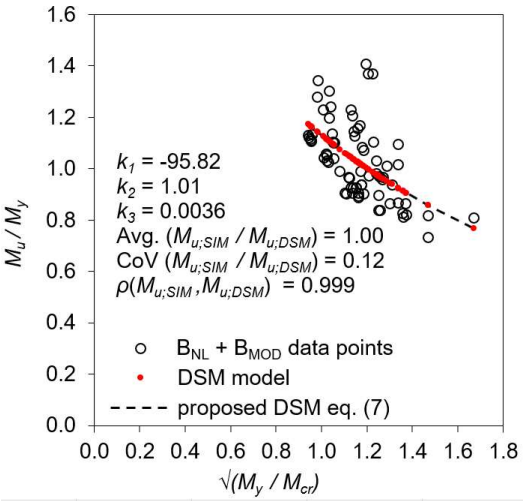

Figure 9: DSM-B; equation 7 [2] for pure bending.

The somewhat high CoV for web crippling is investigated further by conducting ITF web crippling simulations. This may be useful, as ITF simulations do not include a bending moment, and their Eigenmodes are related to buckling of the web instead of the flange. For the derivation of the DSM-W equation, now for the Eigenvalue and yield load either the IOF or ITF value can be used. Resulting correlations between the ultimate loads of the (IOF) simulations and the DSM-W equation are found in table 3. All variants perform worse than the original situation.

Table 3: CoV ($F_{u;SIM}$ / $F_{u;DSM}$) for different combinations with the IOF and ITF yield and critical loads.

	IOF F_{cr}	ITF F_{cr}
IOF F_y	0.19	0.21
ITF F_y	0.24	0.26

For the last step in the interaction DSM approach, the standard format of an interaction rule for combined bending and web crippling is given by eq. 2. In this equation, F is the actual load to be checked for web crippling against F_u, and M the actual bending moment to be checked against the ultimate bending moment M_u. The presence of combined loading is considered by the factors a and b. For a three-point bending test with load $P_{u;IR}$, the bending moment M in eq. 2 can be rewritten as $1/4P_{u;IR}(L_{span} - L_{lb})$ and the concentrated load F can be replaced by load $P_{u;IR}$, resulting in equation (3).

$$a\frac{F}{F_u} + b\frac{M}{M_u} \leq 1 \wedge \frac{F}{F_u} \leq 1 \wedge \frac{M}{M_u} \leq 1 \qquad (2)$$

$$\frac{1}{\frac{a}{F_u} + \frac{b\left(L_{span} - L_{lb}\right)}{4M_u}} \geq P_{u;IR} \qquad (3)$$

The ultimate concentrated loads F_u from the W_{NL} model and the ultimate bending moments M_u from the B_{NL} model are used as input to calibrate the factors a and b. The factors a and b are varied untill a minimum square error was attained between P_u (the ultimate load of the C_{NL} model) and $P_{u;IR}$.

The F_u and M_u values as predicted by the DSM-W and DSM-B equations can be inserted in the derived interaction rule, resulting in the $P_{u;DSM}$ as predicted by the interaction DSM approach. For this, a CoV of 0.13 is obtained between $P_{u;DSM}$ and P_u. Figure 10 presents the results (red markers), including the results of the explicit DSM approach from section 5.1 (black markers). In Figure 11 the results of the interaction DSM approach are given in the interaction space.

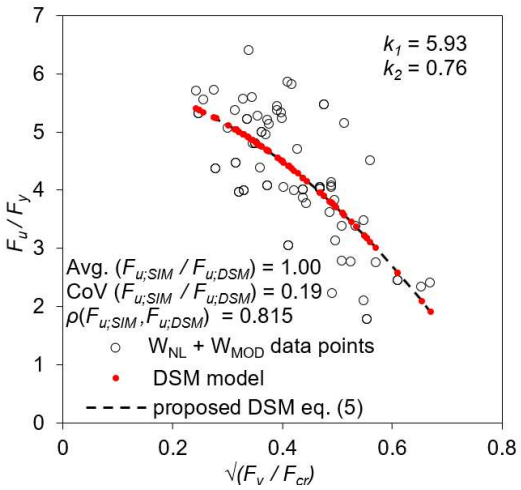

Figure 10: DSM-W; equation 5 [2] for IOF web crippling.

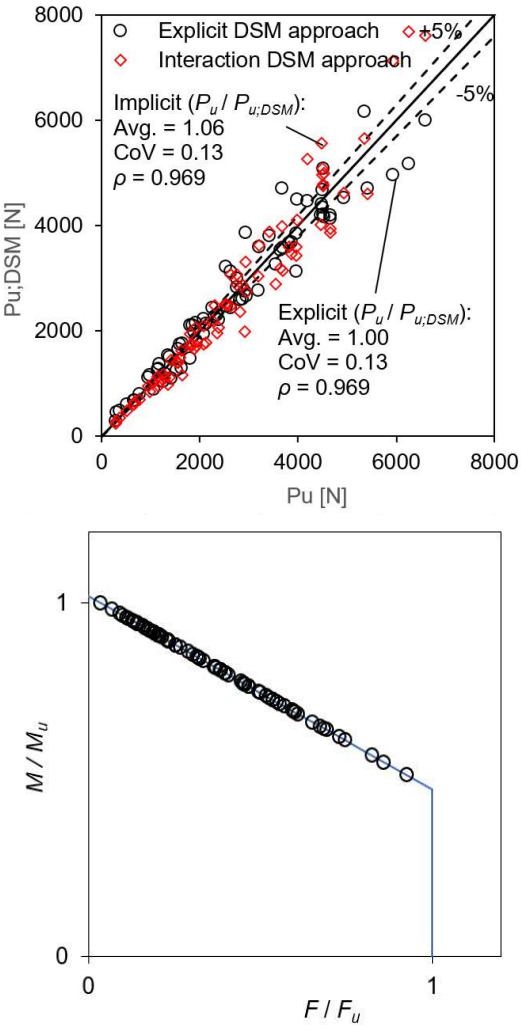

Figure 11: Visualisation of the outcomes of the explicit and the interaction DSM approaches (top), and results interaction DSM approach given in interaction space (bottom).

6. Comparisons

6.1 Current design rules

To assess the developed DSM approaches further, they can also be compared with the current design rules. The web crippling load and the interaction rule for combined load are determined with two different design rules: (i) Eurocode EN1993-1-3 [12] and (ii) The North American Specification for the Design of Cold-Formed Steel Structural Members AISI S100-16 [10].

To calculate the web crippling load, Eurocode EN 1993-1-3 [12] only provides equations for sheeting with at most 1 stiffener in the web. Therefore, for sheeting with more stiffeners in the web, an interpretation of the equations is made [13].

For IOF web crippling, the correlation between the ultimate loads of the simulations F_u and the predicted loads by the Eurocode $F_{u;EC3}$ are presented in figure 12 for sections with 0 or 1 stiffener, and in figure 13 for two or three stiffeners in the web. Striking is that Eurocode results are better for 1 or 2 stiffeners than without. For three stiffeners only 2 cases exist, so conclusions should not be made.

For combined actions, the Eurocode predictions for web crippling are used together with the ultimate bending moment M_u obtained in the simulations in the Eurocode interaction rule, as shown in figure 14 and 15 for 0 and 1, and 2 and 3 stiffeners respectively. Although the CoV is higher for 2 stiffeners than for the other groups, overall the CoV seems to be useable.

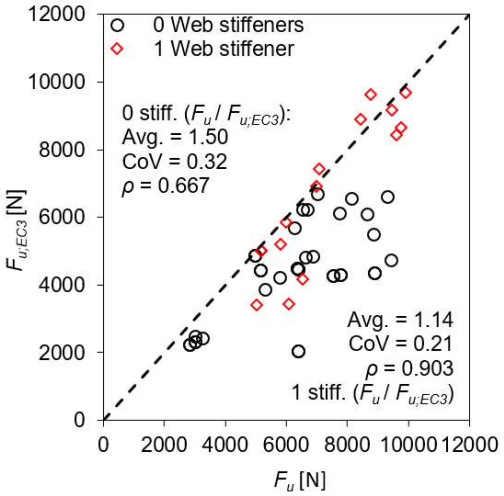

Figure 12: Comparison of web crippling loads predicted by Eurocode 3 and the W_{NL} model for sheeting with 0 or 1 stiffener in the web.

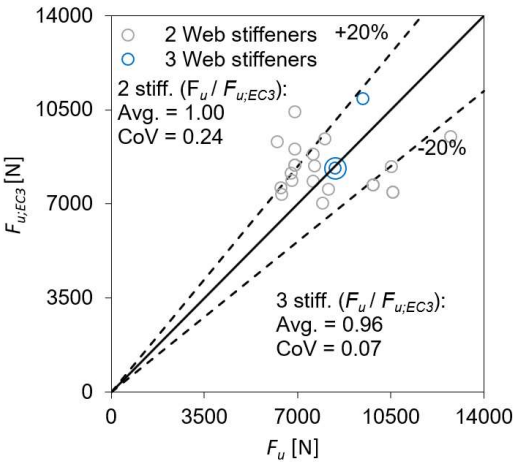

Figure 13: Comparison of web crippling loads predicted by Eurocode 3 and the W_{NL} model for sheeting with 2 or 3 stiffeners in the web. Correlation is negative, so not displayed.

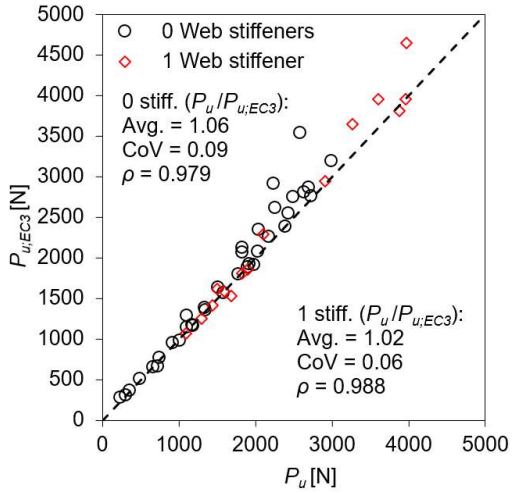

Figure 14: Comparison of ultimate loads predicted by Eurocode 3 and the C_{NL} model for sheeting with 0 or 1 stiffener in the web.

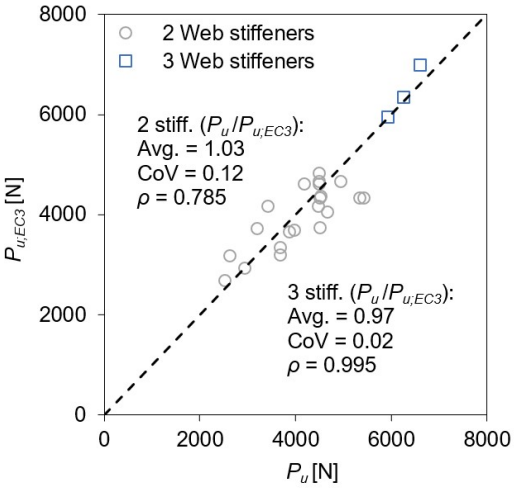

Figure 15: Comparison of ultimate loads predicted by Eurocode 3 [12] and the C_{NL} model for sheeting with 2 or 3 stiffeners in the web.

The AISI S100-16 [10] only provides web crippling equations for sheeting without stiffeners in the web. The performance with a CoV = 0,28 (see figure 16) is a little better than the Eurocode predictions (CoV = 0.32, see figure 12). When applying the interaction rule of the S100-16 (see figure 17), again good results are obtained, similar to the Eurocode.

7. Conclusions

Explicit and interaction DSM approaches have been developed for combined bending and web crippling of second-generation trapezoidal steel sheeting. The explicit DSM approach performs well with a CoV equal to 0.13. Using an alternative yield load did not change the results, probably because only 4 out of 78 simulations were suspectable to instabilities before the yield load. For the interaction DSM approach, separate DSM equations were developed for pure bending and IOF web crippling. The DSM equations for web crippling did not perform very well for 0 stiffeners in the web, with a CoV equal to 0.19. However, the results were still better than the current design rules for web crippling; Eurocode3 (CoV = 0.32) and AISI S100 (CoV = 0.28). Using ITF Eigenvalues and ITF yield loads did not improve the CoV values. Overall, the interaction DSM approach performed well for the numerical experiments, with a CoV equal to 0.13, but not better than Eurocode3 (CoV = 0.09) and the AISI S100 (CoV = 0.15).

The presented DSM approaches are promising, but to further verify the finite element simulations, more experiments are needed. Also, the set of numerical experiments should be further extended with other sheeting types, and more span lengths and load bearing plate widths.

If the DSM is to be used without a linear finite element simulation, which delivers the yield load here, a practically derivable yield load is needed. As such, a simplified ultimate failure model, as presented in the introduction, could still serve a role.

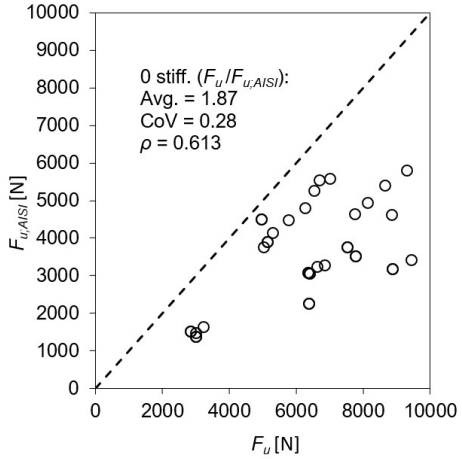

Figure 16: Comparison of the web crippling load predicted by the AISI S100-16 and the W_{NL} model, for sheeting without stiffeners in the web.

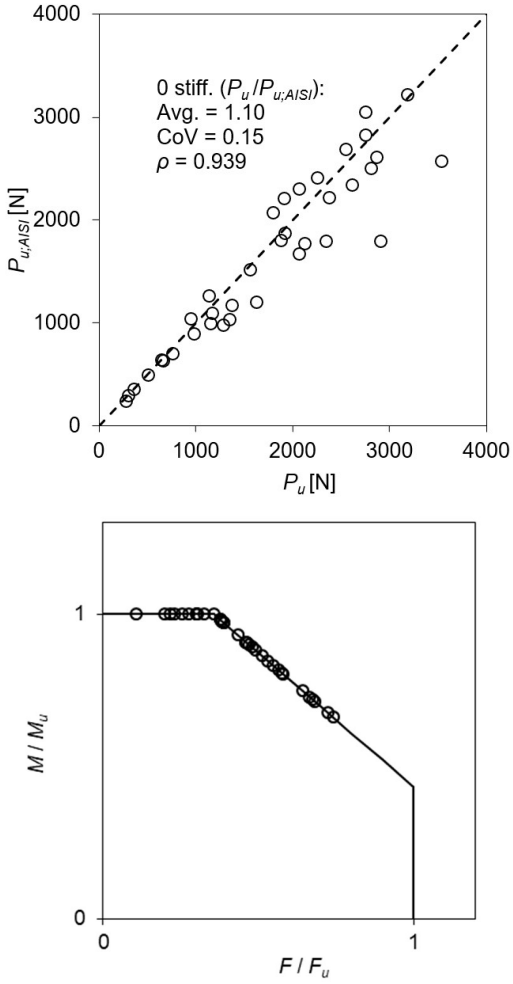

Figure 17: Comparison of the ultimate loads for combined action as predicted by the AISI S100-16 and the C_{NL} simulation model (only for sheeting with no stiffeners in the web) (top), and results given in interaction space (bottom).

References

[1] Hofmeyer, H., Kerstens, J.G.M., Snijder, H.H., Bakker, M.C.M. (2002). Combined web crippling and bending moment failure of first-generation trapezoidal steel sheeting, Journal of Constructional Steel Research 58, 1509–1529.

[2] Zakhimi, H., Hofmeyer, H., Snijder, H.H., Mahendran, M. (2020). Explicit and Interaction Direct Strength Methods for Combined Web Crippling and Bending Moment Failure of First-Generation Trapezoidal Steel Sheeting, Thin Walled Structures 157, 106927.

[3] Marguerre, K. (1938). Zur Theorie der gekrümmter Platte grosser Formänderung. In: Proceedings of the 5th International Congress for Applied Mechanics, September 12-26, Harvard/Cambridge, 93-101.

[4] Hofmeyer, H.; Rosmanit, M.; Bakker, M.C.M. (2009). Prediction of sheeting failure by an ultimate failure model using the fictitious strain method, Thin-Walled Structures 47, 151-162.

[5] Hofmeyer, H., Kaspers, M., Snijder, H.H., Bakker, M.C.M. (2002). Ultimate failure behaviour of second-generation sheeting subjected to combined bending moment and concentrated load. In: International Specialty Conference on Cold-Formed Steel Structures, Orlando, Florida, USA, 109–126.

[6] Franco, J.M.S., Batista, E. de M. (2017). Buckling behavior and strength of thin-walled stiffened trapezoidal CFS under flexural bending, Thin-Walled Structures 117, 268–281.

[7] Casariego, P., Casafont, M., Ferrer, M., Marimon, F. (2019a). Analytical study of flat and curved trapezoidal cold formed steel sheets by means of the yield line theory, Part 1: Flat sheets without transverse corrugations, Thin-Walled Structures 141, 675–692.

[8] Casariego, P., Casafont, M., Ferrer, M., Marimon, F. (2019b). Analytical study of flat and curved trapezoidal cold formed steel sheets by means of the yield line theory, Part 2: Curved sheets with transverse corrugations, Thin-Walled Structures 141, 693–712.

[9] Dassault Systemes (2019). Abaqus 6.12, Dassault Systemes, Vélizy-Villacoublay, France, www.3ds.com/ products-services/simulia/products/abaqus.

[10] AISI (2016). American Iron and Steel Institute, North American specification for the design of cold-formed steel structural members, Cold-formed Steel Design Manual, AISI S100-16, Washington, USA.

[11] Hofmeyer, H., Vervoort, E.M.C., Snijder, H.H., Maljaars, J. (2018). Representativeness of compressed flange behaviour for trapezoidal steel sheeting under combined web crippling and bending. In: Proceedings Eight International Conference on Thin-Walled Structures ICTWS 2018, July 24-27, 2018, Lisbon, Portugal.

[12] CEN European Committee for Standardization (2006). EN 1993-1-3:2006, Eurocode 3: Design of steel structures - part 1-3: General rules - Supplementary rules for cold-formed steel members and sheeting, Brussels, Belgium.

[13] Willems, D.W.C., Hofmeyer, H., Snijder, H.H., Schafer, B.W. (2020). The Direct Strength Method for Combined Bending and Web Crippling of Second-Generation Trapezoidal Steel Sheeting, to be submitted to Thin-Walled Structures.